creative commons
COMMONS DEED

저작자표시-비영리-변경금지 2.0 대한민국

이용자는 아래의 조건을 따르는 경우에 한하여 자유롭게

- 이 저작물을 복제, 배포, 전송, 전시, 공연 및 방송할 수 있습니다.

다음과 같은 조건을 따라야 합니다:

저작자표시. 귀하는 원저작자를 표시하여야 합니다.

비영리. 귀하는 이 저작물을 영리 목적으로 이용할 수 없습니다.

변경금지. 귀하는 이 저작물을 개작, 변형 또는 가공할 수 없습니다.

- 귀하는, 이 저작물의 재이용이나 배포의 경우, 이 저작물에 적용된 이용허락조건을 명확하게 나타내어야 합니다.
- 저작권자로부터 별도의 허가를 받으면 이러한 조건들은 적용되지 않습니다.

저작권법에 따른 이용자의 권리는 위의 내용에 의하여 영향을 받지 않습니다.

이것은 이용허락규약(Legal Code)을 이해하기 쉽게 요약한 것입니다.

Disclaimer

dCollection

이학석사 학위논문

조절된 식각과정에 의한 Eu^{3+}도핑된 속 빈 구조의 Gd_2O_3 나노입자의 합성

Synthesis of Eu^{3+}-doped Gd_2O_3 in hollow nanoparticle structures by controlled chemical etching with poly(acrylic acid)

2012 년 8 월

서울대학교 대학원

화학부 무기화학

유 성 민

조절된 식각과정에 의한 Eu^{3+}도핑된 속 빈 구조의 Gd_2O_3 나노입자의 합성

Synthesis of Eu^{3+}-doped Gd_2O_3 in hollow nanoparticle structures by controlled chemical etching with poly(acrylic acid)

지도 교수 이 진 규

이 논문을 이학석사 학위논문으로 제출함

2012 년 8 월

서울대학교 대학원

화학부 무기화학

유 성 민

유성민의 이학석사 학위논문을 인준함

2012 년 8 월

위 원 장	남 좌 민	(인)
부위원장	이 진 규	(인)
위 원	손 병 혁	(인)

Abstract

Synthesis of Eu^{3+}-doped Gd_2O_3 in hollow nanoparticle structures by controlled chemical etching with poly(acrylic acid)

SungMin Yu

Department of Chemistry

College of Natural Science

Seoul National University

Hollow Eu^{3+}:Gd_2O_3 nanoparticles were easily prepared from the spherical crystalline Eu^{3+}:Gd_2O_3 nanoparticles (NPs) without employing templates by the simple etching process induced by the acidic moieties in the sodium salt solution of poly(acrylic acid), PAA-Na. Some portion of carboxylate units in PAA-Na could bind to the surface of Eu^{3+}:Gd_2O_3 NPs and control the etching rate of Eu^{3+}:Gd_2O_3 in acidic condition to be comparable with the cation migration rate within the crystalline NPs, which could induce Kirkendall effect generating hollow Eu^{3+}:Gd_2O_3 NPs. This controlled etching process in the presence of additional acid after surface treatment of Eu^{3+}:Gd_2O_3 NPs with PAA-Na, could vary the resulted structures from solid NPs to core-shell, core-

void-shell, yolk-shell, and finally to hollow NPs. Based on the small r_2/r_1 value from relaxation times measured by Time-Domain Nuclear Magnetic Resonance (TD-NMR) spectrometer and good photoluminescent property of hollow Eu^{3+}:Gd_2O_3 NPs, it is expected to accelerate development of multimodal nanoprobes and drug delivery vessels using various morphological novelty of synthesized Eu-doped Gd_2O_3 nanoparticles.

Keywords : Hollow Gd_2O_3, Chemical etching method, Multimodal nanoprobe, T_1 contrast agent, Atomic emission.

Student Number : 2010-23094

Table of contents

Abstract 1

List of Figures and Tables..... 4

Introduction 8

Experimental Section 11

Result and Discussion.....15

Conclusion 38

References 40

Abstract (in Korean) 43

Acknowledgement 45

List of figures and Tables

Figure 1. TEM and SEM images of Eu^{3+}:$Gd(OH)CO_3 \cdot H_2O$ nanoparticles with various sizes of (a, d) 60 nm, (b, e) 100 nm, and (c, f) 140 nm, respectively.

Figure 2. (a) TEM images of 90 nm-sized solid Eu^{3+}:Gd_2O_3 nanoparticles. (b) photoluminescent images of amorphous Eu^{3+}:$Gd(OH)CO_3.H_2O$ nanoparticles and solid Eu^{3+}:Gd_2O_3 nanoparticles. (c) The XRD patterns after annealing at different temperatures of 350°C (blue), 450°C (red), and 550°C (black) for 2 h(*ICDD no. 00-043-1014* for pure Gd_2O_3 crystal).

Figure 3. (a) Excitation and (b) emission spectra of Gd_2O_3-based nanoparticles; The corresponding photoluminescence spectra of amorphous 4% Eu^{3+}:$GdOH(CO_3) \cdot H_2O$ nanoparticles (black line) and solid 4% Eu^{3+}:Gd_2O_3 nanoparticles (red line).

Figure 4. (a) TEM image of hollow Eu^{3+}:Gd_2O_3 NPs with ED pattern(inset image), (b) SEM image of hollow Eu^{3+}:Gd_2O_3 nanoparticles.

Figure 5. Photoluminescence spectra of solid Eu^{3+}:Gd_2O_3 nanoparticles (excitation : black line, emission : red line) and hollow Eu^{3+}:Gd_2O_3 nanoparticles (excitation : blue line, emission : green line).

Figure 6. (a) XRD pattern of hollow NPs (black line) and the reference pattern of Gd_2O_3 (green bars). (b) The difference between hollow NPs (black line) and solid NPs (red line) based on the measurement by TGA-DSC.

Figure 7. TEM images of etched Eu^{3+}:Gd_2O_3 NPs in (a) slightly-etched (1 h), (b) core-shell (2 h), (c) core-void-shell (3 h), (d) yolk-shell (7.5 h), (e) hollow (12 h), and (f) fragmented structures (4 days), respectively. Scale bars in the high magnification images are shown with 50 nm size.

Figure 8. The etched amounts of Gd^{3+} in the supernatants with different reaction times by using ICP-AES.

Figure 9. TEM images of products after heating at 70 ^{o}C for 5 h with different amounts of PAA-Na. the relative weight ratio of PAA-Na to Eu^{3+}:Gd_2O_3 NPs was (a) 10 and (b) 30.

Figure 10. TEM images of etched Eu^{3+}:Gd_2O_3 NPs after heating at 70 ^{o}C; (a) for 15 min at *p*H 6.6, (b) for 5 h at *p*H 7.6, and (c) for 5 h at *p*H 8.5.

Figure 11. (a) TEM image of slightly-etched Eu^{3+}:Gd_2O_3 NPs after treating with 25 times excess PAA-Na at room temperature for 7 h, TEM images after the excess amount of PAA-Na was removed and the slightly-etched Eu^{3+}:Gd_2O_3 NPs were (b) further heated at 70 ^oC for 20 h, and (c)-(e) further reacted with acetic acid at room temperature for 30 min in different concentrations of 1, 10, and 100 mM, respectively, (f) TEM image of randomly-etched Eu^{3+}:Gd_2O_3 NPs after directly treating with 10 mM acetic acid at room temperature for 6 h.

Figure 12. TEM images of the randomly etched NPs using acetic acid (a), EDTA (b), and aspartic acid (c).

Scheme 1. Schematic illustration to compare the etching processes of Eu^{3+}:Gd_2O_3 NPs in acidic condition (a) with and (b) without over-coating of PAA-Na.

Figure 13. (a) the result of Dynamic Light Scattering (DLS) and (b) the zeta potential of Hollow NPs.

Figure 14. The plots of T_1 and T_2 relaxation time of hollow Eu^{3+}:Gd_2O_3 nanoparticles as a function of total concentration of Gd and Eu (corresponding calculated r_1 and r_2 values were shown).

Table 1. Reported relaxivity data of representative Gd_2O_3-based T_1 contrast agents

Introduction

Hollow nanoparticles (NPs) have attracted much interest due to the large surface area and pore volume compared to solid nanoparticles having no inner voids. Their potential for encapsulating molecules within the empty core space makes them a good candidate as drug delivery carriers.[1-3] In addition to that kind of application, for the magnetic NPs with the growing attention in the magnetic resonance imaging (MRI) techniques, the inner void space of the hollow NPs is expected to enlarge the surface area of the MR-active paramagnetic centers, which have been investigated by many researches as a good candidate for effective T_1 contrast agent.[4-6]

For past decades, owing to the valuable researches on the MRI contrast agent, MRI became more powerful and precise tool for diagnosis in the medical research field.[7-10] There are two kinds of contrast agents for enhancing contrast effect as T_1-positive and T_2-negative agents. However, T_2 contrast agent can cause the confusion in the clinical usage due to the dark signal induced by the negative enhancement of T_2 contrast agent which is similar to other pathogenic conditions.[11] Due to this reason, T_1 agent is more suitable than T_2 agent for the usage as a contrasting agent and several gadolinium

complexes have already been widely used.[8-10] However, it has been known that molecular MRI contrast agents in a metal complex form have some disadvantages like short life time and fast tumbling rate. On the other hand, nanoparticles (NPs) are expected to have better ability for the T_1-enhancement; the better interaction with water molecule with large surface area, increased payloads of paramagnetic metal ions in the surface, and long life time in the body.[11,12] With an expectation of advantages in nanostructured materials, there have been a lot of researches on the gadolinium oxide (Gd_2O_3) NPs because Gd is not only the most popular candidate with paramagnetic nature and strong T_1 relaxation effect, arising from its seven unpaired electrons in the 4*f* shell,[13-17] but also its oxide, Gd_2O_3, is widely known as a good host material for the optical imaging when doped with lanthanide family metal ions. [18-21] Therefore, by doping with other lanthanide metal ion to tune the photoluminescent color, MRI active Gd_2O_3 can be used as a dual mode imaging nanoprobe.

Although there were a lot of known synthetic methods for various Gd_2O_3 NPs, it has not been reported to synthesize hollow Gd_2O_3 NPs without employing templates. All the reported methods of preparing hollow Gd_2O_3 NPs were template-mediated approaches using gelatin,[22] hydrothermal carbon

spheres (HTCs),[23] melamine formaldehyde (MF),[24,25] and silica shell.[15] However, template-mediated approaches always have several disadvantages such as complex synthetic processes to prepare and remove the template, possible contamination with impurities, structural changes, and some limitations to make small size hollow NPs.[26]

Herein, we reported the easy and simple synthetic method to generate hollow Eu^{3+} ion-doped Gd_2O_3 (Eu^{3+}:Gd_2O_3) NPs without employing templates via the chemical etching process by using a sodium salt of poly(acrylic acid) (PAA-Na). Both the crystallinity showing a good photoluminescence and the hollow structure of Eu^{3+}:Gd_2O_3 NPs could make it very promising to use them as a dual-mode imaging nanoprobe for fluorescence and MRI analyses.

Experimental section

Chemicals and instrumentation.

$GdCl_3 \cdot 6H_2O$, $EuCl_3 \cdot 6H_2O$, and sodium salt of poly(acrylic acid) (PAA-Na) were purchased from Sigma Aldrich. Urea was purchased from Samchun Chemical. All the chemicals were used as received without further purification. Scanning electron microscopy (SEM) was conducted using Hitachi S-4300. Transmission electron microscopy (TEM) image was obtained using Hitachi H-7600 and Jeol 2100 alternatively. Photoluminescence (PL) spectra were measured with Photoluminescence spectrometry, JASCO FP-6500.

Synthesis of Eu^{3+}:$Gd(OH)CO_3 \cdot H_2O$ NPs.

1.5 g of urea was completely dissolved in 290 ml of deionized water by ultra-sonication and stirring and the solution was heated to 90 °C. When the temperature of the solution reached at 90 °C, the mixture of $GdCl_3 \cdot 6H_2O$ (0.48 g) and $EuCl_3 \cdot 6H_2O$ (0.02 g) in 10 ml of deionized water was injected to the hot urea solution. The temperature of the reaction mixture was maintained at 90 °C for 2 h. After cooling the reaction mixture with ice bath, white precipitates were separated by centrifugation and washed with deionized

water several times. The size of collected NPs was about 100 nm with a narrow size distribution. By changing the relative ratio of urea and metal sources, the size of generated Eu^{3+}:$Gd(OH)CO_3 \cdot H_2O$ NPs was precisely controlled; 1.5:3.0 and 4.0:0.5 (wt. ratio) of urea and metal chloride mixture produced 60 and 140 nm NPs, respectively.

Synthesis of solid Eu^{3+}:Gd_2O_3 NPs.

To obtain 90 nm size crystalline Eu^{3+}:Gd_2O_3 NPs, ~100 nm size amorphous Eu^{3+}:$Gd(OH)CO_3 \cdot H_2O$ NPs were dried under vacuum and the dried powder was grinded finely with mortar, and they were annealed in the furnace (heated to 550 ^oC within 1 h and maintained for 2 h). The annealed powder product was grinded with mortar again and ultra-sonicated in water to dispersed solution.

Synthesis of hollow Eu^{3+}:Gd_2O_3 NPs.

To 2.5 mL of PAA-Na aqueous solution (50 mg/mL) preheated to 70 ^oC, 5 mL of the dispersed solution of Eu^{3+}:Gd_2O_3 NPs (1 mg/mL aqueous solution) was slowly added. After appropriate periods of reaction times from 1 to 12 h, etched products were isolated by centrifugation and washed several times with

water to give various structures of etched Eu^{3+}:Gd_2O_3 NPs from core-shell, core- void - shell, yolk-shell, and finally hollow-spherical structures.

Optical Characterization.

Photoluminescent excitation and emission spectra for solid and hollow NPs were measured with Photoluminescence spectrometry, JASCO FP-6500.

Transmission Electron Microscopy (TEM) and Scanning Electron Microscopy (SEM).

Samples for Transmission Electron Microscopy (TEM) were prepared by loading several drops of dilute water dispersion of the particles on amorphous carbon-coated copper grids and drying under room temperature in air. Their images were obtained using Hitachi H-7600 and Jeol 2100 TEM operating at an accelerating voltage of 100 kV and 200 kV, respectively, to analyze the size, size distribution, and the morphology of various nanoparticles. For Scanning Electron Microscopy (SEM) analysis, one drop of dilute water dispersion was loaded on a piece of silicon wafer and drying under room temperature in air. The measurements were carried out with a Hitachi S4300 SEM.

Powder X-ray Diffraction.

Powder XRD was performed New D8 Advance diffractometer (Bruker) in reflection geometry using Cu Kα radiation (1.5405 Å). Measurements were performed in a 2θ range from 10˚ to 80˚. Nanoparticles were precipitated with centrifugation and dried under vacuum overnight for sample preparation of XRD measurements.

MRI relaxation time measurement.

T_1 and T_2 relaxation times of the Eu^{3+}:Gd_2O_3 hollow NPs with various concentrations were measured using 0.47 T Time-Domain Nuclear Magnetic Resonance (TD-NMR, Minispec) spectrometer. The T_1 inversion recovery relaxation time application information was that the number of data points for fitting was 20 with first pulse separation (20 ms) and final pulse separation (5000 ms). And the application information for the T_2 relaxation time was that total 200 data points for fitting was measured with 90^o – 180^o pulse separation (1 tau). We derived relaxivities based on the molar concentration of gadolinium and europium atoms measured by ICP-AES.

Results and Discussion

Synthesis of Eu^{3+}:Gd_2O_3 NPs.

As an extended investigation of the previously reported synthetic method of Gd_2O_3 NPs,[15] Eu^{3+}-doped $Gd(OH)CO_3{\cdot}H_2O$ NPs {Eu^{3+}:$Gd(OH)CO_3{\cdot}H_2O$} were prepared and the size could be controlled in the range of 60~140 nm with a narrow distribution by injecting the mixed metal source of $GdCl_3$ and $EuCl_3$ into the preheated urea solution at 90 ºC (Figure 1).

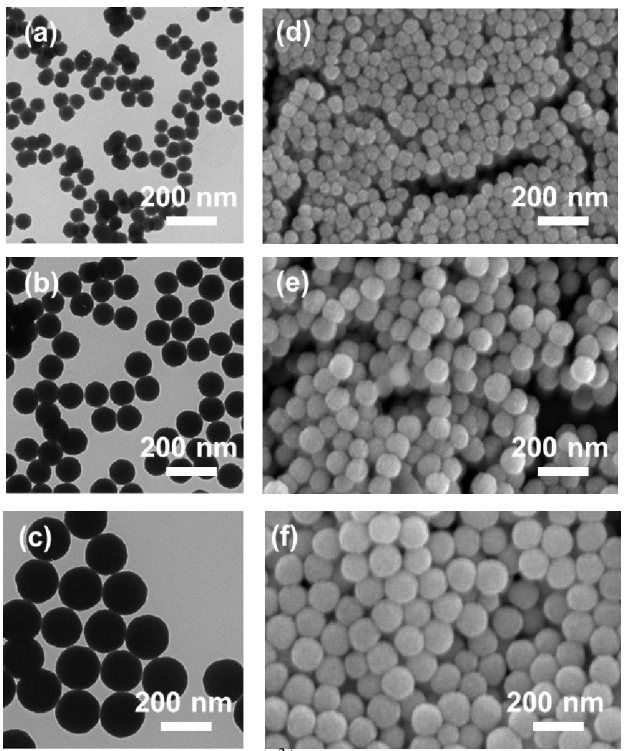

Figure 1. TEM and SEM images of Eu^{3+}:$Gd(OH)CO_3{\cdot}H_2O$ nanoparticles with various sizes of (a, d) 60 nm, (b, e) 100 nm, and (c, f) 140 nm, respectively.

Based on the literature, the optimal doping ratio of Eu^{3+} was set to 4 % for better luminescent property.[27] The thermal annealing processes were carried out at different temperature to find out the lowest temperature to effectively generate crystalline Eu^{3+}:Gd_2O_3 NPs from the amorphous Eu^{3+}:$Gd(OH)CO_3{\cdot}H_2O$ NPs because the energy transfer from oxygen to europium in atomic level luminescence was not effective in amorphous phase.[18,28] From the XRD measurements of annealed products at different temperature as shown in Figure 2, the optimum annealing condition was selected as heating to 550 ºC within 1 h and maintaining at that temperature for 2 h.

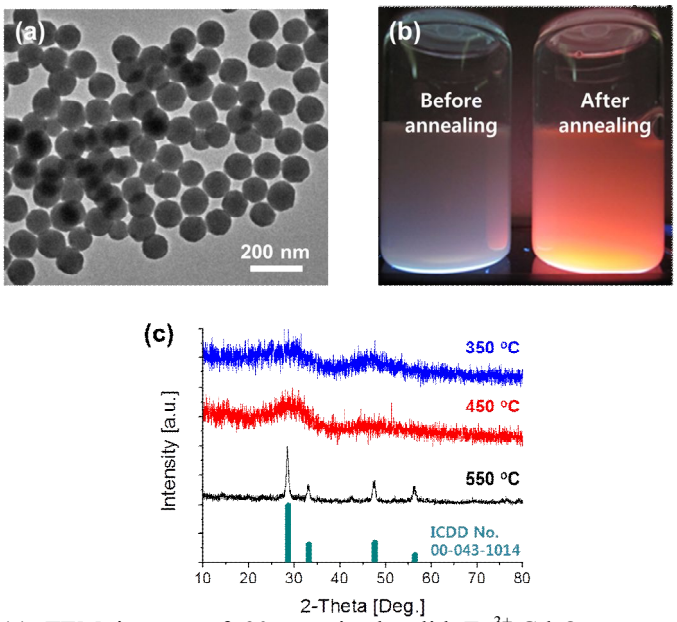

Figure 2. (a) TEM images of 90 nm-sized solid Eu^{3+}:Gd_2O_3 nanoparticles. (b)

photoluminescent images of amorphous Eu^{3+}:$Gd(OH)CO_3.H_2O$ nanoparticles and solid Eu^{3+}:Gd_2O_3 nanoparticles. (c) The XRD patterns after annealing at different temperatures of 350°C (blue), 450°C (red), and 550°C (black) for 2 h(*ICDD no. 00-043-1014* for pure Gd_2O_3 crystal).

The enhanced photoluminescence was clearly observed after annealing at 550 ºC as shown in Figure 1b. Several sharp lines in the excitation spectrum of the amorphous Eu^{3+}:$Gd(OH)CO_3 \cdot H_2O$ NPs at 364, 383, 396, 414, 465, and 536 nm which were corresponded to the direct excitation of europium *f* electrons were decreased significantly comparing to the charge-transfer band (from oxygen to europium) at 264 nm in the excitation spectrum of crystalline Eu^{3+}:Gd_2O_3 NPs (Figure 3). This phenomenon indicates that the improved crystalline structure allows the most efficient energy transfer from the oxygen of the host Gd_2O_3 to the activator Eu^{3+} ions as reported in the literature.[18,21,28]

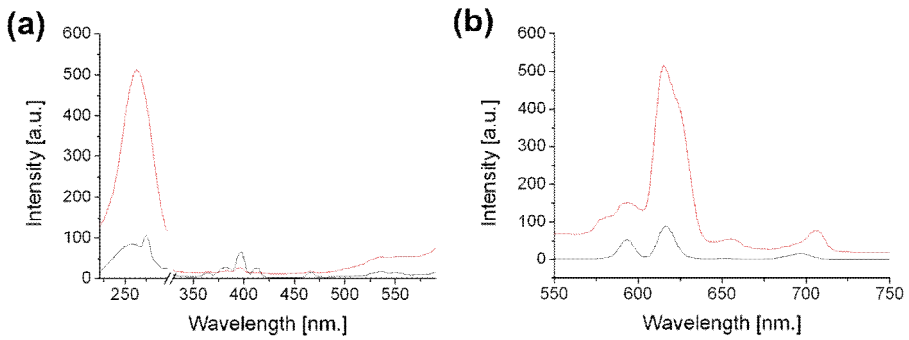

Figure 3. (a) Excitation and (b) emission spectra of Gd_2O_3-based nanoparticles; The corresponding photoluminescence spectra of amorphous 4% Eu^{3+}:$GdOH(CO_3) \cdot H_2O$ nanoparticles (black line) and solid 4% Eu^{3+}:Gd_2O_3 nanoparticles (red line).

Generation of hollow Eu^{3+}:Gd_2O_3 NPs with PAA-Na.

Although photoluminescence was clearly enhanced after annealing at 550 ºC, Eu^{3+}:Gd_2O_3 NPs were not stably dispersed in polar solvents such as water and alcohols even after grinding and agitating with ultrasonication. Therefore, a well-known surface-treating polyelectrolyte such as sodium salt of poly(acrylic acid), PAA-Na, was employed to increase the dispersibility of Eu^{3+}:Gd_2O_3 NPs in water; several carboxylate units within polymer chains are expected to bind to the positive metallic site on the surface of NPs. PAA-Na could slightly enhance the dispersion stability, but most of Eu^{3+}:Gd_2O_3 NPs were precipitated within 1 h probably due to the relatively high density (7.07 g/ml for bulk Gd_2O_3). Interestingly, when an excess amount of PAA-Na (25 times excess by weight compared to Eu^{3+}:Gd_2O_3) were used and heated at 70 ºC for 12 h, the turbidity of the solution decreased significantly and the dispersion stability seemed to be enhanced a lot. Transmission electron microscope (TEM) and scanning electron microscope (SEM) images revealed that the resulted material had a hollow structure as shown in Figure 4.

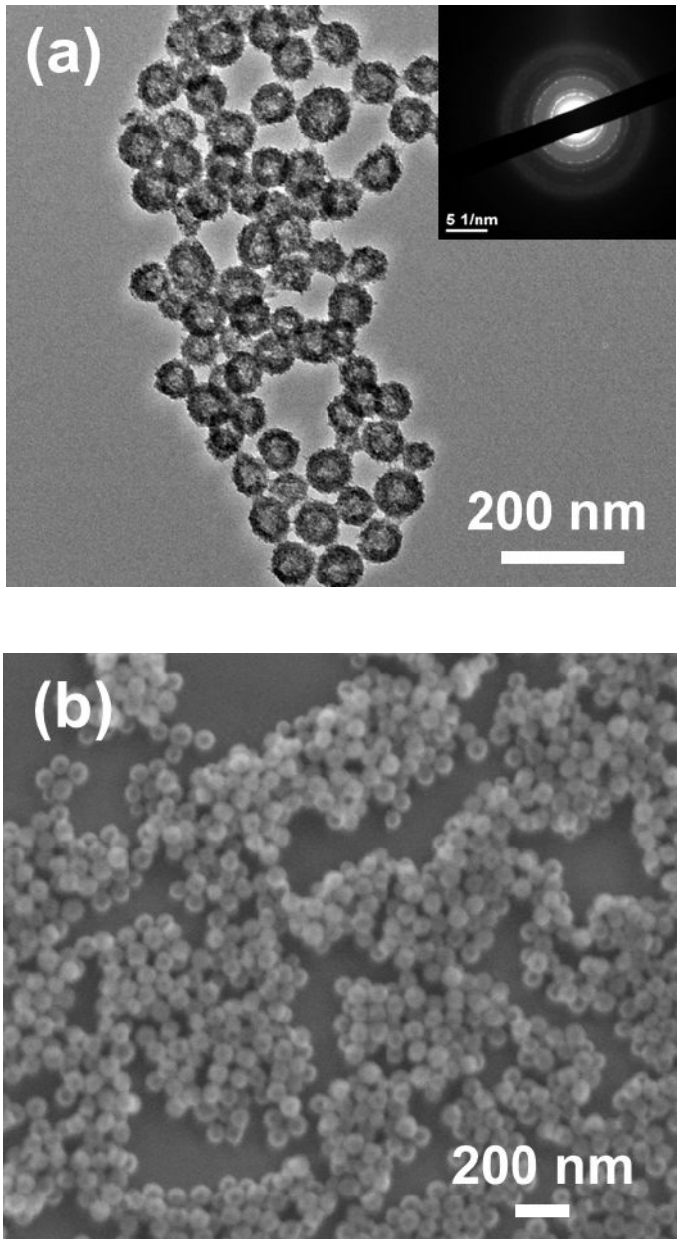

Figure 4. (a) TEM image of hollow Eu^{3+}:Gd_2O_3 NPs with ED pattern(inset image), (b) SEM image of hollow Eu^{3+}:Gd_2O_3 nanoparticles.

The crystallinity seemed to be maintained in this hollow Eu^{3+}:Gd_2O_3 NPs based on the well-developed polycrystalline electron diffraction patterns in Figure 4a and photoluminescent excitation and emission spectra also showed no significant changes, confirming the crystallinity of hollow Eu^{3+}:Gd_2O_3 NPs (Figure 5).

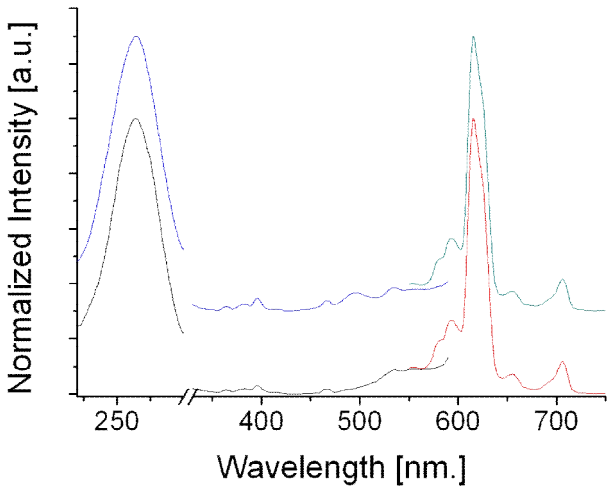

Figure 5. Photoluminescence spectra of solid Eu^{3+}:Gd_2O_3 nanoparticles (excitation : black line, emission : red line) and hollow Eu^{3+}:Gd_2O_3 nanoparticles (excitation : blue line, emission : green line).

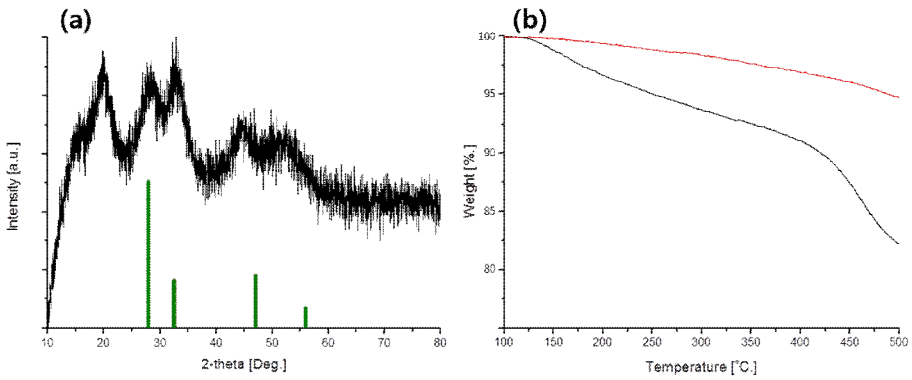

Figure 6. (a) XRD pattern of hollow NPs (black line) and the reference pattern of Gd_2O_3 (green bars). (b) The difference between hollow NPs (black line) and solid NPs (red line) based on the measurement by TGA-DSC.

In addition to the polycrystalline property in the figure 4a and the proof that the hollow NPs are maintained as cubic-phase Gd_2O_3 as shown in the unchanged charge-transfer bands of the figure 5, we have confirmed XRD pattern of hollow NPs to check for the exact crystallinity and compared solid NPs with hollow NPs in the different tendency under high temperature by using TGA-DSC (Figure 6). Corresponding to the results of Figure 4a and 5, in the XRD result, there were not only the characteristic peaks of Gd_2O_3 but also two peaks related to the PAA in 18.4 ^{o} and 32.0 ^{o}. [29] The broad pattern of PAA including two unique peaks made it difficult to understand the overall XRD pattern, because some peaks for Gd_2O_3 were overlapped with the broad pattern of the polymer. So, because we have made sure that the complex

pattern resulted from the over-coated PAA-Na on the surface of hollow NPs, we confirmed the experiment using TGA-DSC to compare the tendencies of solid and hollow NPs under increasing temperature (Figure 6b). Because in the initial stage for the preparation of solid NPs, annealing temperature was 550 ^{o}C, we selected the temperature range from 100 to 500 ^{o}C to prevent confusion with the result induced by the crystallization at 550 ^{o}C. From the results in the figure 6, we could understand the the complex pattern in the XRD is attributed to the PAA-Na that surround the hollow NPs on the surface.

In order to understand the generation of the hollow Eu^{3+}:Gd_2O_3 NPs, the changes in Eu^{3+}:Gd_2O_3 NPs was monitored by TEM after different heating times at 70 ℃.

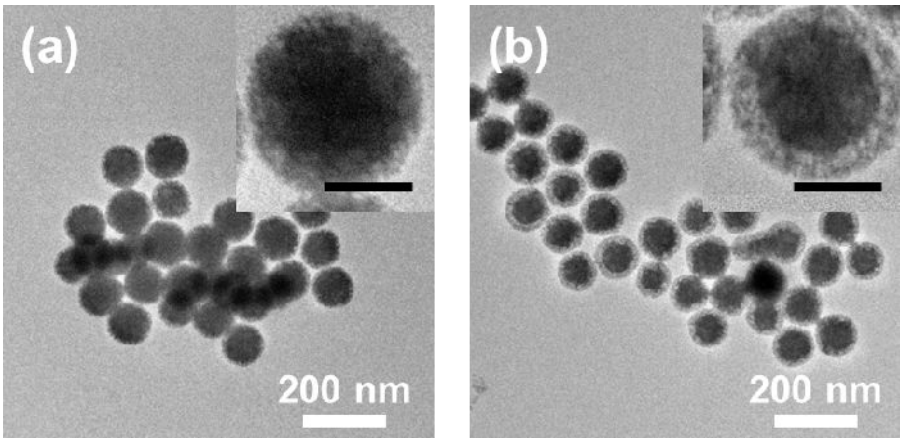

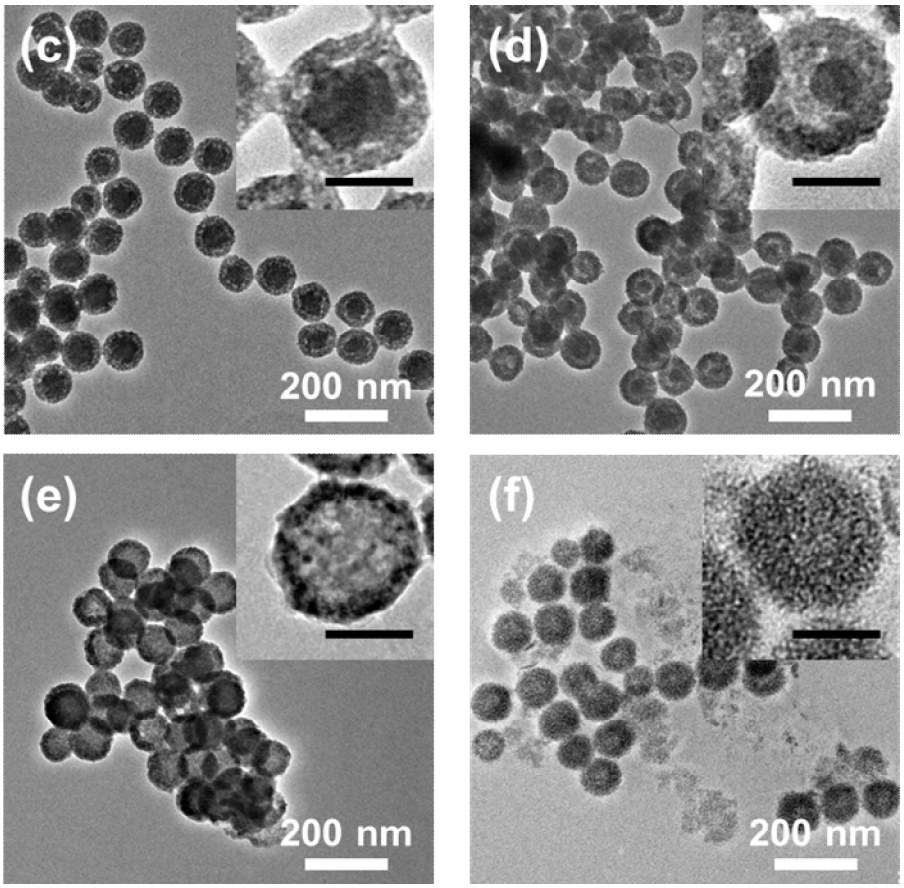

Figure 7. TEM images of etched Eu^{3+}:Gd_2O_3 NPs in (a) slightly-etched (1 h), (b) core-shell (2 h), (c) core-void-shell (3 h), (d) yolk-shell (7.5 h), (e) hollow (12 h), and (f) fragmented structures (4 days), respectively. Scale bars in the high magnification images are shown with 50 nm size.

As shown in Figure 7, the surface of nanoparticles started to be etched after 1 h, and core-shell (after 2 h), core-void-shell (after 3 h), york-shell (after 7.5 h), and finally hollow (after 12 h) structures were developed with time; this

behavior is consistent with the typical Kirkendall effect explaining the formation of pores or voids by different diffusion rates of the reactants in alloy systems or oxidation reactions at evaporated temperature.

The reason of void forming in Kirkendall effect is usually explained by outward fast moving of cation through the oxide layer and a balancing inward flow of vacancies to the vicinity of the metal–oxide interface. [3] When Eu^{3+}:Gd_2O_3 NPs was heated at 70 ºC for 4 days, many NPs lost the hollow structure and were divided into small fragments which had been reported as a critical consequence of etching process in several nanoparticle systems. [4]

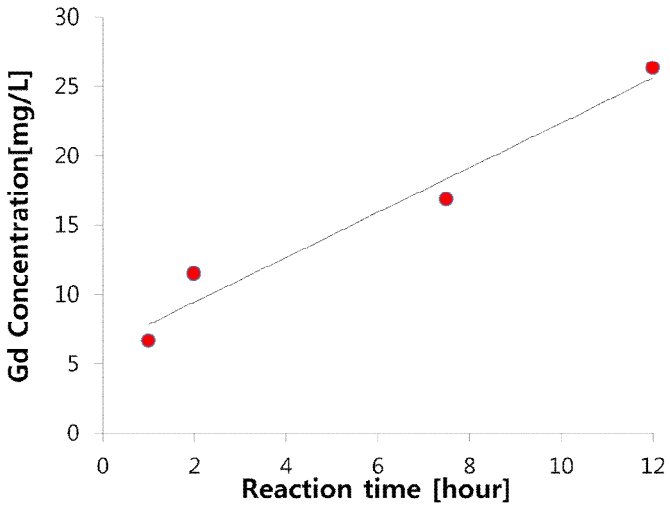

Figure 8. The etched amounts of Gd^{3+} in the supernatants with different reaction times by using ICP-AES.

The etched amount of Gd^{3+} in the supernatants after the appropriate reaction times of 1, 2, 7.5, and 12 h was measured by ICP-AES, and the summarized results (Figure 8) showed that the concentration of Gd^{3+} in the supernatants was increased as a function of reaction time indicating that these phenomena should be based on the etching process.

From these time-dependent results, it was speculated that hollow nanostructure was generated by acid moiety in PAA-Na which might be left over owing to the incomplete conversion with a strong base such as NaOH or might be produced by contacting with CO_2 in the air during the storage. When the relative weight ratio of PAA-Na to Eu^{3+}:Gd_2O_3 NP was changed to 10 or 30 (comparing to 25 in the case of Figure 7) and the mixed solutions were heated at 70 ℃ for 5 h, the etching rate seemed to be proportional to the amount of PAA-Na (Figure 9).

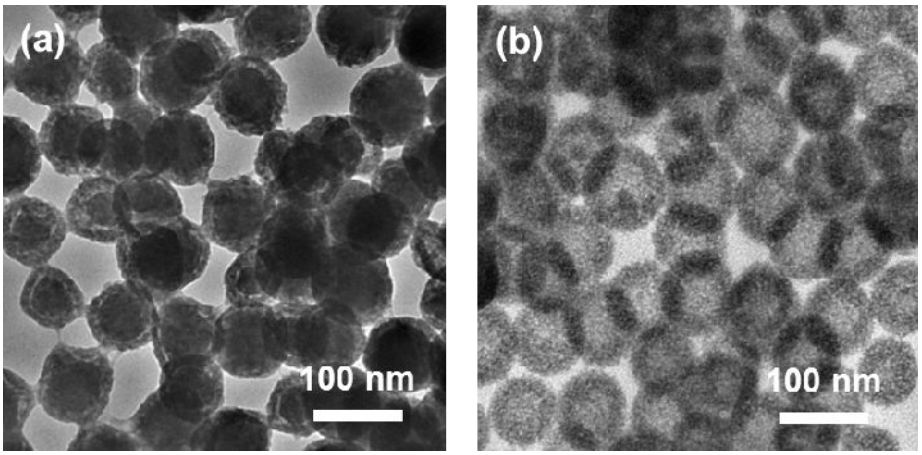

Figure 9. TEM images of products after heating at 70 °C for 5 h with different amounts of PAA-Na. the relative weight ratio of PAA-Na to Eu^{3+}:Gd_2O_3 NPs was (a) 10 and (b) 30.

In the case of 10 times excess amount of PAA-Na, the generated structure looked like an early stage of core-void-shell formation which seemed to be in the intermediate situation between structures after 2 h (Figure 7b) and 3 h (Figure 7c) in 25 times excess case. On the other hand, in the case of 30 times excess amount of PAA-Na, the complete hollow structure was only observed.

In order to confirm that the acid moiety in PAA-Na played a main role of etching process, similar etching reactions with PAA-Na at different *p*Hs were carried out at 70 ℃. Even though the amount of acid moiety was not perfectly controlled as in buffered solutions, the *p*H of as-received PAA-Na solution was measured as 7.9 and it could be tuned by adding 1 M acetic acid and 1 M

sodium hydroxide solutions to get various PAA solutions with *p*Hs of 6.6, 7.6, and 8.5, respectively. As expected, in the case of *p*H 6.6, the mixed solution turned to be almost transparent after 15 min and TEM revealed the formation of hollow Eu^{3+}:Gd_2O_3 NPs (Figure 10a).

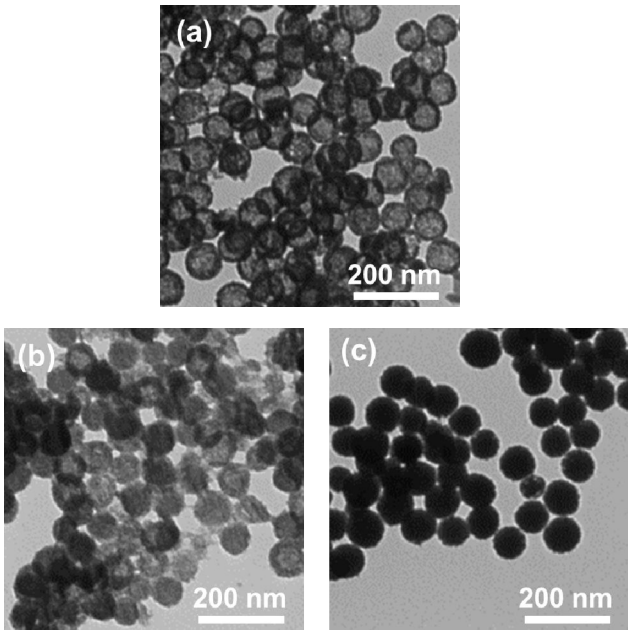

Figure 10. TEM images of etched Eu^{3+}:Gd_2O_3 NPs after heating at 70 ^oC; (a) for 15 min at *p*H 6.6, (b) for 5 h at *p*H 7.6, and (c) for 5 h at *p*H 8.5.

In the case of *p*H 7.6, etching rate seemed to be slightly faster to produce hollow structures compared to the structure generated after 12 h in the normal etching condition of *p*H 7.9 (Figure 10b), while there were no significant

changes even 5 h of heating at *p*H 8.5 (Figure 10c). Furthermore, when poly(acrylic acid) was purchased and directly treated with Eu^{3+}:Gd_2O_3 NPs with a weight ratio of 25 at room temperature, the solution turned to be transparent without showing any scattering owing to the nanoparticles within 1 h which was almost same as the case of using acetic acid to dissolve away Eu^{3+}:Gd_2O_3 NPs.

When the relative weight ratio of PAA-Na to Eu^{3+}:Gd_2O_3 NP was fixed to 25 as in the case of Figure 7 but the mixed solutions were kept at room temperature for 7 h, the surface was slightly etched as shown in Figure 11a.

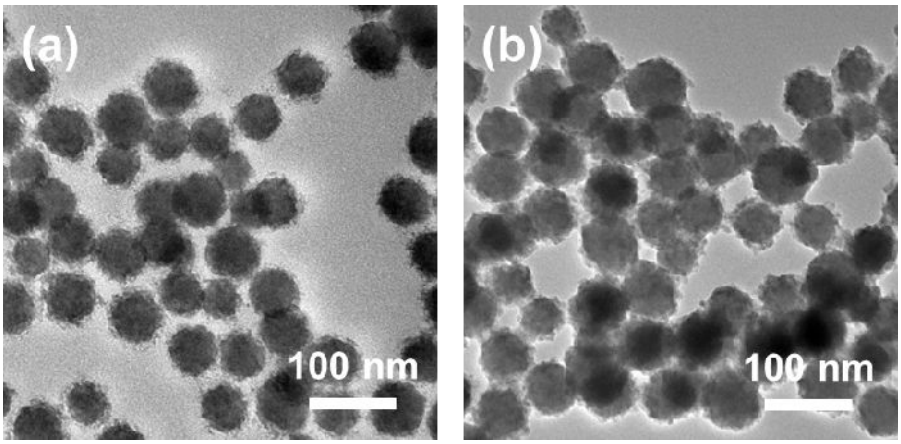

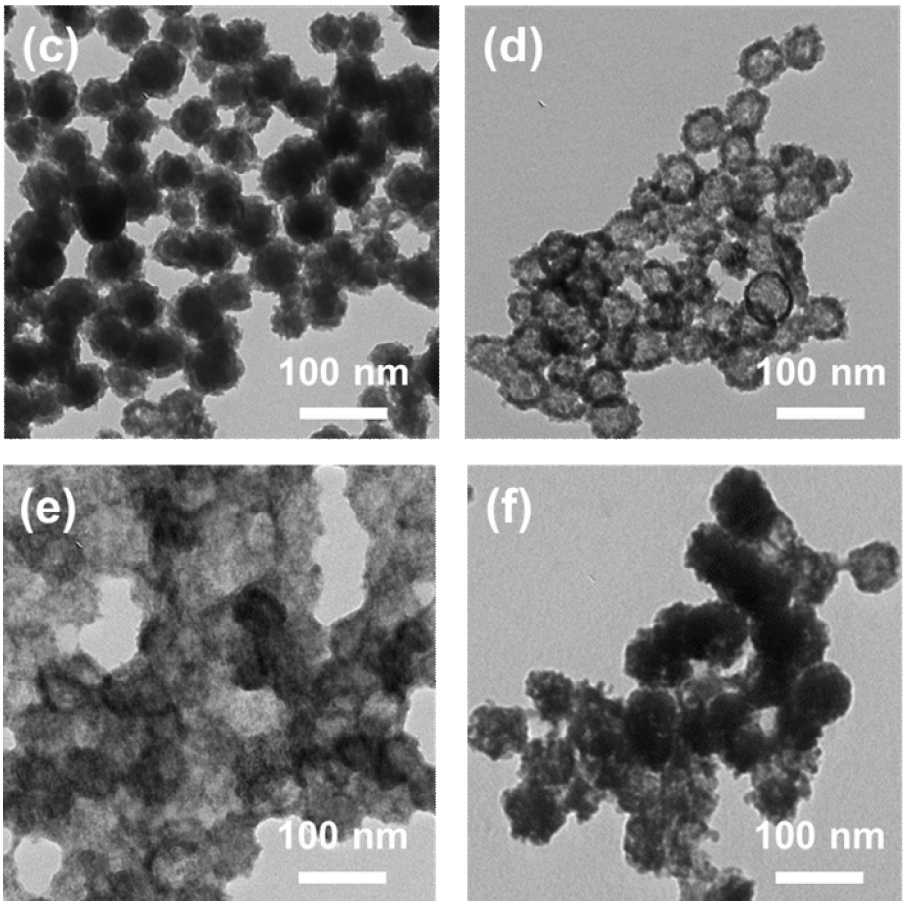

Figure 11. (a) TEM image of slightly-etched Eu^{3+}:Gd_2O_3 NPs after treating with 25 times excess PAA-Na at room temperature for 7 h, TEM images after the excess amount of PAA-Na was removed and the slightly-etched Eu^{3+}:Gd_2O_3 NPs were (b) further heated at 70 ^{o}C for 20 h, and (c)-(e) further reacted with acetic acid at room temperature for 30 min in different concentrations of 1, 10, and 100 mM, respectively, (f) TEM image of randomly-etched Eu^{3+}:Gd_2O_3 NPs after directly treating with 10 mM acetic acid at room temperature for 6 h.

The excess amount of PAA-Na was removed from the slightly etched Eu^{3+}:Gd_2O_3 NPs by centrifugation and they were redispersed in water to be heated at 70 ºC. As shown in Figure 11b, even after 20 h of heating, no detectable changes were observed, confirming again that acid moiety from the excess amount of PAA-Na plays critical role in etching process to generate hollow NPs. When acetic acid was introduced as an acid source into the re-dispersed solution of slightly etched Eu^{3+}:Gd_2O_3 NPs, etching process began to proceed again even at room temperature as a function of acid concentration. From the case of 1 mM of acetic acid as shown in Figure 11c, the core-void-shell structure was mainly generated after 30 min. When the concentration of acetic acid was increased, the etching process was accelerated as expected to generate the hollow structure from 10 mM of acetic acid while almost fragmented structures were developed from 100 mM of acetic acid as shown in Figure 11d and e, respectively. If acetic acid was added into the dispersed solution of Eu^{3+}:Gd_2O_3 NPs without being over-coated with PAA-Na, it seemed like that the etching could not start effectively at the beginning step but it proceeded too fast not to maintain the spherical shape and to generate hollow structure even after 6 h in 10 mM condition (Figure 11f).

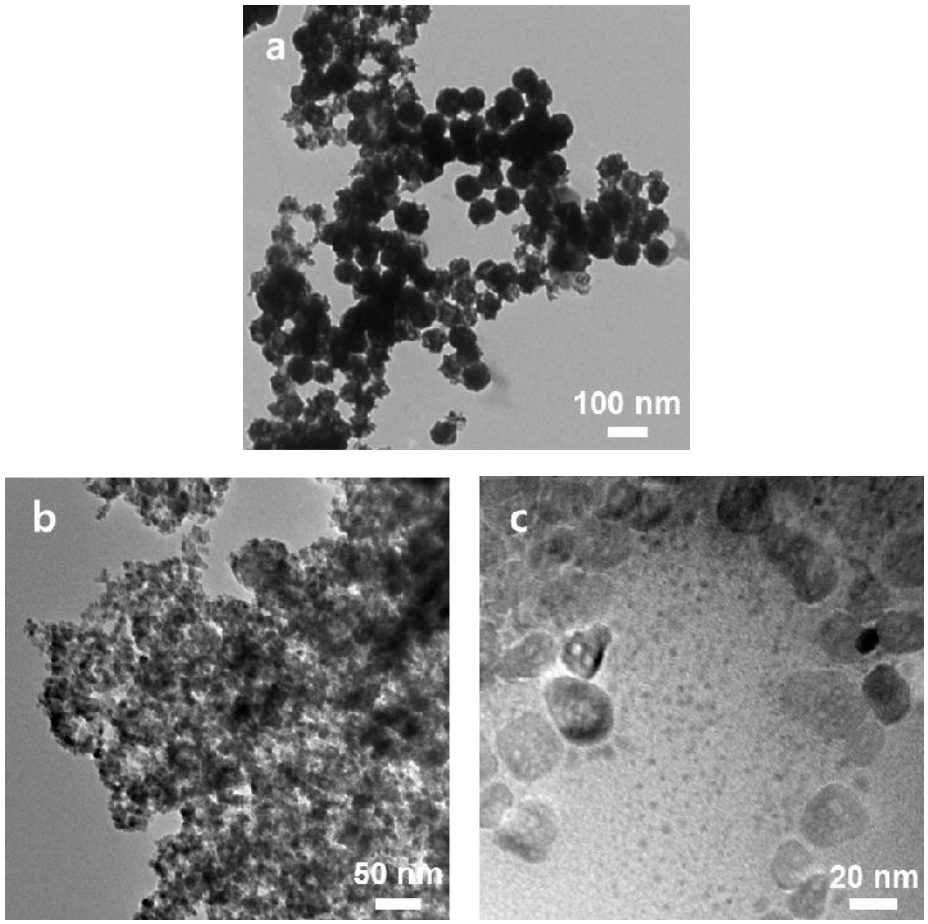

Figure 12. TEM images of the randomly etched NPs using acetic acid (a), EDTA (b), and aspartic acid (c).

As mentioned above in the figure 11f, when we used single molecule acids as etchants, the particles were randomly etched without uniformity in their morphology (figure 12). It seems that the etching process with single

molecule acids is too fast to stabilize the morphology of particles thermodynamically, because the ability of single molecule acids as stabilizers cannot be enough to compensate the rate of dissolution to the reaction system by the relatively faster etching process through the single molecule acids.

Therefore, the role of PAA-Na is most likely to bind to the cationic metal sites on the NP surface and to reduce the diffusing rate of M^{3+} into the solution. As a consequence with these important roles of PAA-Na, the etching rate of Eu^{3+}:Gd_2O_3 is reduced to be comparable with the cation migration rate within the crystalline NPs to induce Kirkindall effect generating hollow Eu^{3+}:Gd_2O_3 NPs. Without over-coating with PAA-Na, etched M^{3+} ions could be easily diffused into the solution to accelerate the etching speed owing to the increased surface area at the etched sites. It resulted in the irregular shape of etched NPs and no hollow structure can be generated as explained in Scheme 1.

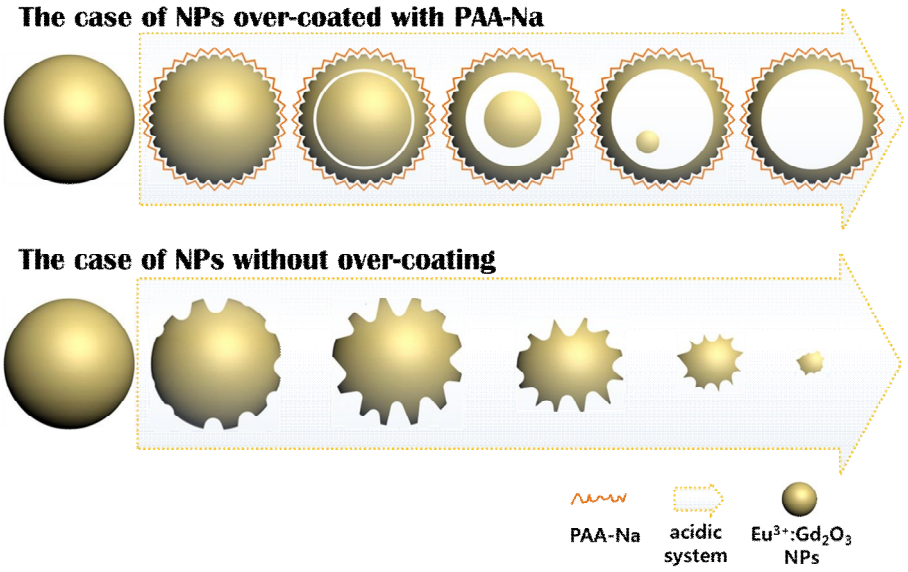

Scheme 1. Schematic illustration to compare the etching processes of Eu^{3+}:Gd_2O_3 NPs in acidic condition (a) with and (b) without over-coating of PAA-Na.

In the first step of the reaction in the presence of PAA-Na, it chelates to metal sites on the surface of solid NPs and acidic units of PAA-Na acts as an etchant. It causes the vacancies on the surface but the random etching rate is reduced by the chelation of PAA. In the meantime, metal ions in the inner core part diffuse to those vacancies to fill while protons migrate into the core in relatively much faster speed.

Therefore the rate determining step seems to be the diffusion rate of etched M^{3+} into the solution which can be controlled by the chelation of PAA on the NP surface. As time passes, vacancies keep being generated to form void and the inner core gets smaller. Accordingly, the morphology changes from solid NPs to core-shell, core-void-shell, yolk-shell, and finally to hollow NPs step-by-step.[4,5]

Characteristic features of hollow Eu^{3+}:Gd_2O_3 NPs as a dual mode imaging nanoprobe.

Beside of the above mentioned characteristic photo-luminescent property of the hollow Eu^{3+}:Gd_2O_3 NPs (Figure 2b and Figure 5), the inner void space of the hollow structure is expected to enlarge the surface area of the MR-active paramagnetic centers, which have been investigated by many researches as a good candidate for an effective T_1 contrast agent.[4-6] The spin relaxation property of hollow NPs dispersed in deionized water was measured using 0.47 T (Tesla) Time-Domain Nuclear Magnetic Resonance (TD-NMR, minispec) spectrometer. In many researches, they often used the agarose gel to measure the T_1 relaxation time, in which it means that the materials are not stable enough to be dispersed in deionized water. However, in our study, while the solid NPs was transformed to the hollow NPs, the dispersibility of the

particles in water was getting better as shown in the Figure 13. It is probably because the PAAs coated on the surface of nanoparticles make the ability enhanced. In the Figure 13a, the result of size distribution induced by hydrodynamic volume is presumably due to the swollen effect of polymer coated on the surface of the NPs in the solvent. And in the Figure 13b, the result of surface charge measurement using zeta potential shows that the anionic PAA remain well-coated on the surface of NPs.

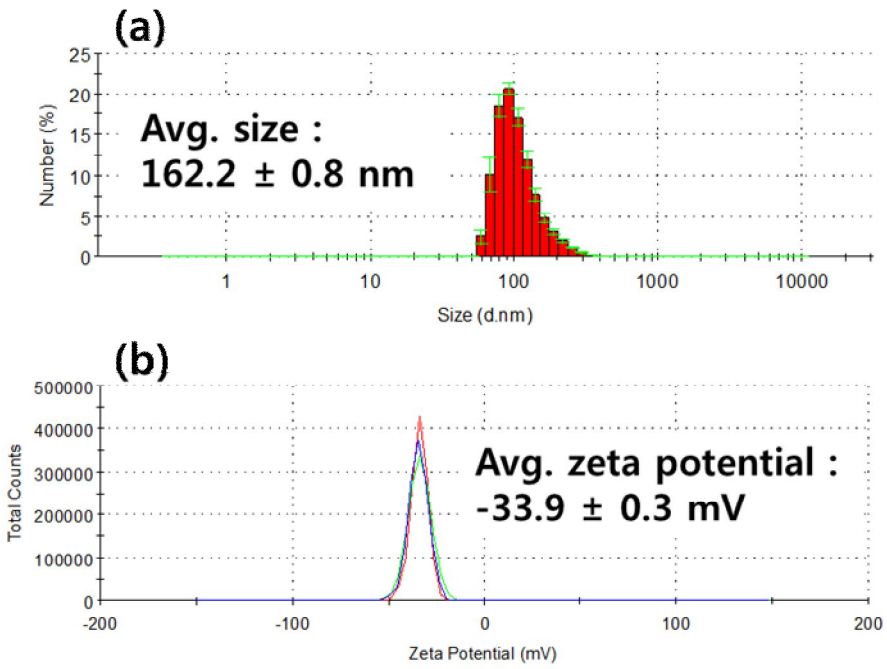

Figure 13. (a) the result of Dynamic Light Scattering (DLS) and (b) the zeta potential of Hollow NPs.

By measuring the variation in relaxation times of samples at different concentrations, the plots of the reciprocal values of relaxation times were obtained as a function of the amount of M^{3+} ions (1/T *vs.* $[M^{3+}]$) and relaxivity values (r_1 and r_2; the slopes of each plot, $mM^{-1}s^{-1}$) were determined as $r_1 = 5.8$ and $r_2 = 9.7$, respectively (Figure 14).

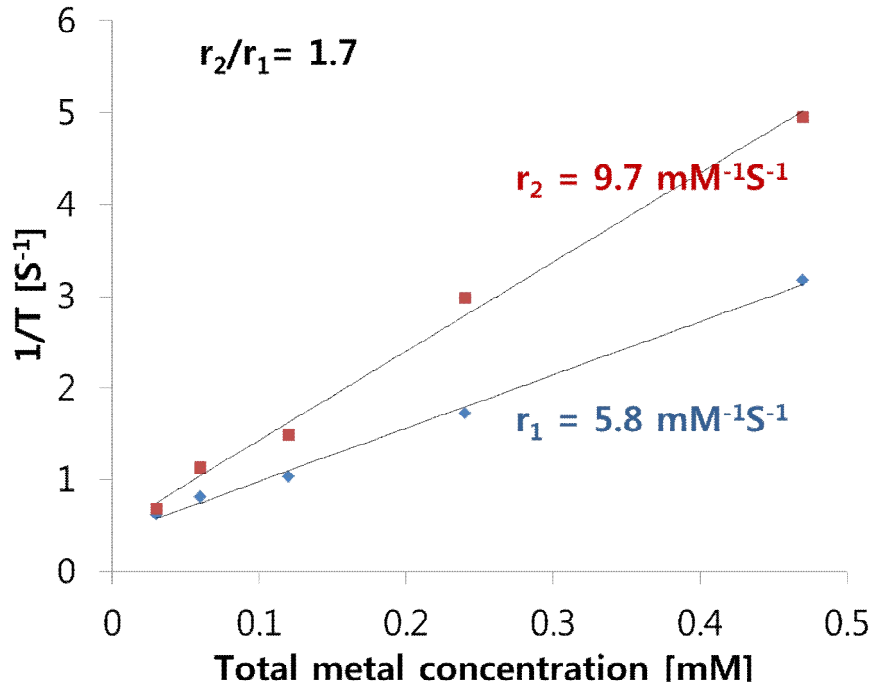

Figure 14. The plots of T_1 and T_2 relaxation time of hollow Eu^{3+}:Gd_2O_3 nanoparticles as a function of total concentration of Gd and Eu (corresponding calculated r_1 and r_2 values were shown).

These relaxivity values are comparable to those of the reported Gd^{3+}-based contrast agents, even though the measured magnetic field strengths were different (Table 1). More interestingly, the r_2/r_1 value of synthesized hollow Eu^{3+}:Gd_2O_3 NPs is calculated as 1.7, suggesting their efficacy as T_1 contrast agents. The relatively high value for r_1 relaxivity is presumably come from the increased surface-to-volume ratio by the interaction between MR active centers in the inner void and water molecules.

Table 1. Reported relaxivity data of representative Gd_2O_3-based T_1 contrast agents

Contrast agent	Diameter (nm)	r_1 ($mM^{-1}S^{-1}$)	r_2 ($mM^{-1}S^{-1}$)	r_2/r_1	B_0(T)	Specific condition	Ref.
Gd_2O_3 (sphere)	~352	22.2	128.9	5.8	3	0.5% agarose gel	16
Gd_2O_3 (cubic-like)	~423x294	19.5	89.4	4.6	3	0.5% agarose gel	16
Hollow Gd_2O_3	~200	17.7	26.6	1.5	3	0.5% agarose gel	22
	~200	2.78	-	-	4.7	0.5% agarose gel	23
Ultra small Gd_2O_3	2.2	8.8	11.4	1.3	7		13
	3.8	8.8	28.8	3.4	7		13
	< 3	9.4	13.4	1.4	1.5		14
	< 40	0.1	7.6	81.6	1.5		14
	1	9.9	10.5	1.1	1.5		17
Tb : Gd_2O_3	~4	12	-	-	1.5		20
Hollow Eu: Gd_2O_3	90	5.9	10.1	1.7	0.47		This work

Conclusion

A simple and easy synthetic method to prepare the hollow Eu^{3+}:Gd_2O_3 NPs without employing templates was developed. The sodium salt of poly(acrylic acid), PAA-Na, could bind the surface of Eu^{3+}:Gd_2O_3 NPs and control the etching rate of Eu^{3+}:Gd_2O_3 in acidic condition to be comparable with the cation migration rate within the crystalline NPs to induce Kirkindall effect generating hollow Eu^{3+}:Gd_2O_3 NPs. Based on the suggested formation mechanism, the hollow Eu^{3+}:Gd_2O_3 NPs could be produced in the presence of additional acid after surface treatment of Eu^{3+}:Gd_2O_3 NPs with PAA-Na. By deliberately controlling the amount of PAA-Na, amount of additional acids, temperature, or etching time, the structure of generated nanoparticles could be varied from solid NPs to core-shell, core-void-shell, yolk-shell, and finally to hollow NPs. The crystallinity of hollow NPs was well-maintained and the dispersion stability of resulted hollow NPs was enhanced dramatically due to the relatively mild reaction condition, it was possible to directly measure the variation in relaxation times of samples at different concentrations even though the overall size was relatively big with an average-size of 90 nm. Based on the small r_2/r_1 value and good photoluminescent property of hollow Eu^{3+}:Gd_2O_3 NPs along with the mild and simple control of morphologies, it is

expected to accelerate development of not only the doped Gd_2O_3 based multimodal nanoprobes but also the drug delivery vessel using various morphological novelty of synthesized nanoparticles.

References

(1) Huang, H.; Remsen, E. E.; Kowalewski, T.; Wooley, K. L. *Journal of the American Chemical Society* **1999**, *121*, 3805.

(2) Sun, Y.; Mayers, B.; Xia, Y. *Advanced Materials* **2003**, *15*, 641.

(3) Yin, Y.; Rioux, R. M.; Erdonmez, C. K.; Hughes, S.; Somorjai, G. A.; Alivisatos, A. P. *Science* **2004**, *304*, 711.

(4) An, K.; Kwon, S. G.; Park, M.; Na, H. B.; Baik, S.-I.; Yu, J. H.; Kim, D.; Son, J. S.; Kim, Y. W.; Song, I. C.; Moon, W. K.; Park, H. M.; Hyeon, T. *Nano Letters* **2008**, *8*, 4252.

(5) Peng, Y.-K.; Lai, C.-W.; Liu, C.-L.; Chen, H.-C.; Hsiao, Y.-H.; Liu, W.-L.; Tang, K.-C.; Chi, Y.; Hsiao, J.-K.; Lim, K.-E.; Liao, H.-E.; Shyue, J.-J.; Chou, P.-T. *ACS Nano* **2011**, *5*, 4177.

(6) Shin, J.; Anisur, R. M.; Ko, M. K.; Im, G. H.; Lee, J. H.; Lee, I. S. *Angewandte Chemie International Edition* **2009**, *48*, 321.

(7) Caravan, P. *Chemical Society Reviews* **2006**, *35*, 512.

(8) Caravan, P.; Ellison, J. J.; McMurry, T. J.; Lauffer, R. B. *Chemical Reviews* **1999**, *99*, 2293.

(9) Hermann, P.; Kotek, J.; Kubicek, V.; Lukes, I. *Dalton Transactions* **2008**, 3027.

(10) Lauffer, R. B. *Chemical Reviews* **1987**, *87*, 901.

(11) Na, H. B.; Song, I. C.; Hyeon, T. *Advanced Materials* **2009**, *21*, 2133.

(12) Na, H. B.; Hyeon, T. *Journal of Materials Chemistry* **2009**, *19*, 6267.

(13) Bridot, J.-L.; Faure, A.-C.; Laurent, S.; Rivière, C.; Billotey, C.; Hiba, B.; Janier, M.; Josserand, V.; Coll, J.-L.; Vander Elst, L.; Muller, R.; Roux, S.; Perriat, P.; Tillement, O. *Journal of the American Chemical Society* **2007**, *129*, 5076.

(14) Fortin, M.-A.; Jr, R. M. P.; Söderlind, F.; Klasson, A.; Engström, M.; Veres, T.; Käll, P.-O.; Uvdal, K. *Nanotechnology* **2007**, *18*, 395501.

(15) Kim, J.; Jung, Y.; Lee, J.-K. *Journal of Nanoparticle Research* **2011**, *13*, 2311.

(16) Li, I. F.; Su, C.-H.; Sheu, H.-S.; Chiu, H.-C.; Lo, Y.-W.; Lin, W.-T.; Chen, J.-H.; Yeh, C.-S. *Advanced Functional Materials* **2008**, *18*, 766.

(17) Park, J. Y.; Baek, M. J.; Choi, E. S.; Woo, S.; Kim, J. H.; Kim, T. J.; Jung, J. C.; Chae, K. S.; Chang, Y.; Lee, G. H. *ACS Nano* **2009**, *3*, 3663.

(18) Goldys, E. M.; Drozdowicz-Tomsia, K.; Jinjun, S.; Dosev, D.; Kennedy, I. M.; Yatsunenko, S.; Godlewski, M. *Journal of the American Chemical Society* **2006**, *128*, 14498.

(19) Guo, H.; Dong, N.; Yin, M.; Zhang, W.; Lou, L.; Xia, S. *The Journal of Physical Chemistry B* **2004**, *108*, 19205.

(20) Petoral, R. M.; Söderlind, F.; Klasson, A.; Suska, A.; Fortin, M. A.; Abrikossova, N.; Selegård, L. a.; Käll, P.-O.; Engström, M.; Uvdal, K. *The*

Journal of Physical Chemistry C **2009**, *113*, 6913.

(21) Seo, S.; Yang, H.; Holloway, P. H. *Journal of Colloid and Interface Science* **2009**, *331*, 236.

(22) Huang, C.-C.; Liu, T.-Y.; Su, C.-H.; Lo, Y.-W.; Chen, J.-H.; Yeh, C.-S. *Chemistry of Materials* **2008**, *20*, 3840.

(23) Tian, G.; Gu, Z.; Liu, X.; Zhou, L.; Yin, W.; Yan, L.; Jin, S.; Ren, W.; Xing, G.; Li, S.; Zhao, Y. *The Journal of Physical Chemistry C* **2011**, *115*, 23790.

(24) Jia, G.; You, H.; Liu, K.; Zheng, Y.; Guo, N.; Zhang, H. *Langmuir* **2009**, *26*, 5122.

(25) Yang, P.; Gai, S.; Liu, Y.; Wang, W.; Li, C.; Lin, J. *Inorganic Chemistry* **2011**, *50*, 2182.

(26) An, K.; Hyeon, T. *Nano Today* **2009**, *4*, 359.

(27) Pires, A. M.; Santos, M. F.; Davolos, M. R.; Stucchi, E. B. *Journal of Alloys and Compounds* **2002**, *344*, 276.

(28) Pang, M. L.; Lin, J.; Fu, J.; Xing, R. B.; Luo, C. X.; Han, Y. C. *Optical Materials* **2003**, *23*, 547.

(29) Bhavana, G.; Rajiv, P. *Materials Science and Engineering: C* **2009**, *29*, 1746.

Abstract

속 빈 구조의 나노입자들은 내부의 빈 공간들로 인해 질량을 줄여 밀도를 낮출 수 있을 뿐만 아니라 그 공간을 이용하여 약물전달시스템에 사용될 수 있는 등의 장점들로 인해 많은 연구들이 진행되어오고 있습니다. 이러한 속 빈 구조의 나노입자를 만드는 다양한 방법 중 생물학적 응용을 위해 합성과정에 지지체를 포함하지 않으며, 그로 인한 불순물 제거과정을 거치지 않는 합성 방법은 하나의 연구주제가 되어오고 있습니다.

본 연구에서는 속이 빈 구형 (hollow sphere)의 Eu^{3+}:Gd_2O_3 나노입자가 지지체 없이, 단순히 고분자인 poly(acrylic acid) 나트륨 염에 소량 존재하는 산 (acid) 부분에 의해 간단한 식각 (etching) 과정을 통해 합성될 수 있었습니다. 이 고분자는 속이 차있는 구형 (solid sphere) 나노입자의 표면에 결합할 수 있고, 산성 조건하에 생기는 Eu^{3+}:Gd_2O_3의 etching 현상에서 그 속도를 조절할 수 있었습니다. 이는 나노입자 표면을 감싸고 있는 고분자가 etching되는 속도와 결정성 있는 입자 내에서의 Kirkendall effect를 가능하게 하는 금속 양이온의 이동속도가 필적할 수 있게

유도되기 때문이었습니다. 이로 인해 내부부터 etching이 일어나는 것 같은 기이한 현상이 발견된다는 것을 확인할 수 있었습니다.

이 고분자와 함께 표면 처리된 Eu^{3+}:Gd_2O_3는 증가하는 산의 농도에 따라 etching 과정을 조절할 수 있었고, 이를 통해 속이 차여져 있는 나노입자로부터 핵-껍질, 핵-공간-껍질, 공 속의 작은 공의 구조, 그리고 마지막으로 속 빈 나노구조로 입자의 구조를 변화시킬 수 있었습니다.

형성된 속 빈 구조의 나노입자의 좋은 photoluminescence property와 Time-domain nuclear magnetic resonance(TD-NMR) spectrometer를 사용하여 측정된 T_1과 T_2 이완시간으로 구해진 작은 r_2/r_1 값을 바탕으로, 합성된 Eu^{3+} 도핑된 Gd_2O_3 나노입자의 형태학적인 진기함을 이용하여 다중방식의 나노프로브와 약물 전달 용기의 개발을 촉진시킬 것으로 기대 되는 연구를 진행하였습니다.

주요어 : Hollow Gd_2O_3, Chemical etching method, Multimodal nanoprobe, T_1 contrast agent, Atomic emission.

학 번 : 2010-23094

Acknowledgment

학부를 졸업하고 대학원생을 꿈꾸며 도전했던 시간들이 엊그제 같은데 벌써 그 시간이 2년 전의 추억이 되었고, 이제는 졸업을 앞둔 시점을 맞이하였다는 것이 실감이 나질 않습니다. 굉장히 빠르게 2년이라는 시간이 지나갔지만, 그 기간 동안 잊지 못할 추억, 경험들이 제게는 또 하나의 보람이 되어 돌아왔습니다. 이렇게 값진 추억과 경험을 할 수 있게 도움을 주신 소중한 분들께 감사의 뜻을 전하고자 합니다.

아직은 어리기 만한 제 인생에 있어서 하고 싶은 것들을 모두 경험할 수 있도록 저를 만들어주시고 믿음으로 이끌어주신 아버지와 어머니께 짧은 글로나마 깊은 감사의 뜻을 전하고 싶습니다. 그리고 항상 곁에서 기쁠 때나 고민이 있을 때 든든한 버팀목이 되어준 세상에 하나 밖에 없는 동생 승현에게도 감사합니다.

제게 대학원 생활을 경험할 수 있도록 길을 열어주신 이진규 교수님께 감사의 마음을 전달하고 싶습니다. 화학을 바탕으로 연구를 해나가는 데 필요한 지식, 문제를 해결해 나가는 데에 있어서의 접근법뿐만 아니라 인생을 살아가는 데에 있어서의 지혜에 대해 생각해볼 수 있는 틀을 제시해주신 부분은 앞으로의 인생을 살아가는 데에 있어서 양질의 밑거름이 될 것 같습니다. 또한 실험실 생활 외적으로도 MT, 등산,

체육활동, home-coming day, 연말행사를 통해 실험실 식구들의 유대감을 돈독히 해주시려는 교수님의 덕으로 또 하나의 가족과 같은 형, 누나, 동생들을 얻을 수 있었던 것 같습니다. 이렇게 재료화학 실험실이라는 하나의 집단에 속해 있었다는 것에 대한 자부심과 잊지 못할 추억을 주신 점 교수님께 두고두고 갚아 나가겠습니다. 그리고 제 논문 심사위원이셨던 손병혁 교수님과 남좌민 교수님께도 감사드립니다.

같은 팀의 리더로서 제게 대학원에서의 실험에 대해 가르쳐 주신 진명이형. 좋은 결과로 박사 후 과정 마무리 잘하시고 앞으로의 진로도 잘 되시길 바라며 감사합니다. 처음에는 실험실에서 옆 테이블에 계셔서 쉽게 다가갈 수 있었지만, 시간이 지나면서 제게 실험뿐만 아니라 그 외적인 고민이 있을 때에도 후배인 제가 쉽게 다가갈 수 있도록 편하게 대해주신 국연이형. 제가 많은 부분에 있어 형 덕에 그것들을 극복하고 이겨나갈 수 있었습니다. 한 학기 힘내셔서 형이 열어둔 가능성들이 모두 실현되시길 바라며 감사의 뜻을 전합니다. 오피스에서 까칠한 도시남자의 풍미를 보이셨던 학성이형. 저는 형의 진심이 뭔지 알고 있습니다. 언제나 후배인 제가 바른 길로 갈 수 있도록 때로는 날카롭게, 때로는 마음이 따뜻한 누나처럼 세심하게 이끌어주신 학성이형, 형의 관심과 후배 사랑 잊지 않고 갚아나가겠습니다. 형의 첫 아기와 형수님 모두 건강하시길, 그리고 형은 좋은 결과로 원하시는 꿈을 이루시길 바라고 응원하겠습니다. 같은

팀의 온화하시지만 가끔은 카리스마를 풍기며 미소 짓게 해주시던 에릭형. 형의 따뜻한 마음과 관심 감사합니다. 현재 실험실 여학우 3인방의 리더이자 MCL의 식구들을 어머니처럼 챙겨주셨던 선배 영재님. 바쁜 방장으로서의 역할을 다하면서도 항상 미소를 잃지 않는 모습이 늘 귀감이 되었습니다. 무뚝뚝하지만, 박학다식하시고 재미있는 여러 취미활동을 즐기시는 두식이형. 부족한 제게 따뜻한 말과 관심, 값진 조언들 모두 너무 감사 드리고, 현재 굉장히 많은 일들을 해내느라 바쁘시겠지만 모두 형에게 좋은 쪽으로 돌아오리라 믿습니다, 힘내세요. 동생이지만 배울 점이 너무나도 많고, TEM 찍어주는 시간을 기다리게 만들어 준 선배 주현님. 실험이 잘 풀리지 않거나 고민할 때, 어떻게 알고 적재적소에 값진 조언과 충고를 아끼지 않아 준 것 너무나 감사합니다. 항상 열심히 노력하는 모습 잘 배워나갑니다. MCL의 early adapter 태근이형. 형수님과 오래오래 행복하시고, 대학원 생활하면서 따뜻하게 대해주시고 관심 주신 것 감사합니다. 형, 꼭 금연 성공하셔요! 대학원 생활을 함께 시작한 동기 정이. 오빠인데도 잘 챙겨주지 못해 미안하고, 마지막까지 바쁜 시간 할애해서 TEM 잘 찍어줘서 고마워. 세포 잘 키워서 좋은 결과 있었으면 좋겠고, 힘들어도 긍정적으로 생각하면서 이겨나가길 바랄게. 실험실 첫 후배이자 든든한 친구 같던 제남이, 그리고 언제 봐도 듬직한 대웅이. 항상 열심히 하고 밝은 너희들이 있어서 웃을 수 있었고 반성하는 계기를 가질

수 있었어. 제남이는 조금만 더 힘내서 다음 학기 잘 마무리 했으면 좋겠고, 대웅이는 지금처럼 긍정적으로 계속 해나가면 문제 없을 거라 생각해. 그리고 실험실의 막내 동생들 사뮤엘 재호 신과 같은 팀의 뭐든 잘하는 잘생긴 지훈이. 아직 후배도 들어오지 않아 여러 일을 도맡아 하지만 지금처럼 항상 열심히 해나가면 모두 좋은 경험이 되어서 값지게 쓰일 거라 생각해. 장난 좋아하는 날 잘 받아줘서 고맙고, 너희들과 지내면서 재미있는 추억들 많이 얻어가는 것 같아, 힘내서 앞으로의 생활도 잘 이겨내 가길 바랄게. 그리고 현재는 졸업하신 MCL의 존재감 연구형, 오래 뵙지는 못했지만 따뜻한 말씀 많이 해주신 유원이형, 같은 동네 사는 친절하신 선화누나, 유쾌한 다정이 모두 감사의 뜻을 전합니다. 그리고 대학원에서 많은 도움을 주시고 큰 힘이 되어주셨으며 친구처럼 많은 시간을 보내주셨던 준상이형 정말 감사합니다.

힘들고 지칠 때 든든한 지원군이 되어준 대현, 철규, 충원, 지훈, 호련, 홍민, 남혁 등 소중한 친구들에게도 감사의 말 전하고, 모두 지금처럼 각자 하는 일 잘 해나가며 우정 변치 않고 지속해나갔으면 좋겠습니다.

다시 한번 저를 믿고 용기를 북돋아주신 우리 가족, 진심으로 사랑합니다. 그리고 조용히 제 옆에서 힘이 되어주고, 잘 맞춰준, 현재는 저의 가장 친한 친구 같은 여자, 사랑하는 박수현. 대학원 생활을 이제 막 시작했지만, 이제는 제가 잘 맞추고 힘이 되어드리겠습니다. 고맙고 사랑합니다.

감사드릴 분이 많지만, 글솜씨가 부족하여 이만 줄일까 합니다. 새로운 도전 앞에서도 이곳에서의 배움과 경험을 잘 활용해서 열심히 살아가도록 하겠습니다. 모든 분들께 진심으로 감사 드리며 행복하시길 바라겠습니다.